A DNA Aptamer Which Binds to and Inhibits Thrombin Exhibits a New Structural Motif for DNA†

Ke Yu Wang,‡ Sarah McCurdy,§ Regan G. Shea,§ S. Swaminathan,*,§ and Philip H. Bolton*,‡

Chemistry Department, Wesleyan University, Middletown, Connecticut 06459, and Gilead Sciences, 346 Lakeside Drive, Foster City, California 94404

Received December 3, 1992; Revised Manuscript Received January 7, 1993

ABSTRACT: The investigation of the three-dimensional structure of the DNA aptamer d($G_1G_2T_3$-$T_4G_5G_6T_7G_8T_9G_{10}G_{11}T_{12}T_{13}G_{14}G_{15}$) which binds to and inhibits thrombin has been carried out by NMR methods. This DNA exhibits a number of long-range NOEs between residues which are not adjacent in sequence, which allowed the determination of the novel tertiary structure adopted. This DNA adopts a highly compact, highly symmetrical structure which consists of two tetrads of guanosine base pairs and three loops. The residues of the tetrads alternate anti–syn–anti–syn. This novel structural motif for DNA may also be relevant to the structure of telomere DNA.

The inhibition of thrombin has therapeutic value in cardiovascular surgery and other settings in which anticoagulation is desired (Salzman, 1992). Acute vascular diseases such as myocardial infarction and cerebral infarction also constitute major health risks in which anticoagulation is desired. Thrombin is a protease which is a key player in the blood coagulation cascade and hence a major target for anticoagulation and vascular disease therapy. At present, heparin is the most widely used anticoagulant. However, the long lifetime of heparin in blood makes it difficult to reverse its anticoagulation activity, and heparin has other unfavorable properties as well. For example, heparin can induce thrombocytopenia and bleeding. Therefore, there has been considerable interest in developing and characterizing a specific thrombin inhibitor which has short lifetime in blood and which exhibits fewer and less severe side effects than heparin (Salzman, 1992). Most of the efforts to find heparin substitutes have focused either on polyanionic sugars related to heparin or on analogues of the naturally occurring peptide inhibitor found in leeches (Salzman, 1992).

An alternative approach has been based on a search for a DNA molecule, or a combination of DNA molecules, which would have the desired thrombin inhibition properties. This search has been carried out using a novel in vitro selection technique (Bock et al., 1992). In this approach 10^{13} different DNA molecules were synthesized and screened for thrombin binding. The DNA molecules were prepared by synthesizing all 60-mers which were flanked by appropriate primers. These DNA molecules were then passed through five rounds of selection and polymerase chain reaction amplification of the selected DNAs. The DNAs with the highest affinity for thrombin, binding constants in the 10 nM range, were sequenced.

The DNA aptamer (Ellington & Szostak, 1990) with the highest reported affinity for thrombin was found to be d($G_1G_2T_3T_4G_5G_6T_7G_8T_9G_{10}G_{11}T_{12}T_{13}G_{14}G_{15}$) (Bock et al., 1992). This DNA aptamer was found to significantly increase the thrombin-catalyzed clotting times of both purified fibrinogen and human plasma and does not compete with known active site inhibitors of thrombin (Bock et al., 1992). The comparison of the sequences of the DNA aptamers which bind most strongly to thrombin indicated that there is a consensus sequence of GGTTGGTNTGGTTGG. It was also found that the DNA hexamer GGTTGG also binds to and inhibits thrombin. The affinity of thrombin for this hexamer is much less than that of the tightest binding aptamer. Thus, we became interested in determining the structure of the DNA aptamer as well as determining whether the structure of the aptamer changes upon binding to thrombin.

Examination of the sequence shows that Watson–Crick base pairing is not possible for this DNA since there are only G and T residues. The presence of G-T wobble base pairs was a possibility but was not considered likely since the aptamer binds to thrombin at 37 °C and G-T base pairs are not thought to offer high thermal stability. As shown below, the aptamer adopts a tertiary structure which is unlike any structure previously documented for DNA.

The sequence of the aptamer is reminiscent of the G_nT_m consensus sequence for telomere DNA. Telomere DNA is located at the ends of eukaryotic chromosomes and is thought to protect the chromosomes and to be needed to overcome the shortening of chromosomes which occurs during replication. Telomere DNA is synthesized by a telomerase, which is a reverse transcriptase. As discussed below, the tertiary structure of the aptamer may be related to that of telomere DNA.

In the Results and Discussion which follow, the NMR-based methods for determining the structure of the aptamer will be presented. While the resonances of this DNA could not be assigned by the conventional sequential assignment strategies used for A- and B-form nucleic acids, there were a sufficient number of long-range connectivities to assign the resonances and a large enough number of NOE connectivities to allow the structure to be determined.

MATERIALS AND METHODS

The DNA aptamer was synthesized by solution-state methods and purified by HPLC. All NMR samples of the aptamer were at a concentration of 150 OD_{260} in the selection buffer containing 0.14 M NaCl, 20 mM perdeuteriated Tris, and 5 mM potassium chloride at a pH of 7.4. All of the NMR

† The research at Wesleyan was supported, in part, by the Patrick and Catherine Weldon Donaghue Medical Research Foundation, Grant NP-750 from the American Cancer Society, and by Gilead Sciences.

‡ Wesleyan University.

§ Gilead Sciences.

0006-2960/93/0432-1899$04.00/0

experiments reported on here were obtained with the sample at 10 °C. Phosphorothioate-labeled samples (Eckstein & Jovin, 1983) were also synthesized by solution-state methods and purified by HPLC. The phosphorothiolate samples contained both diastereomers.

The preliminary characterization of the aptamer by NMR gave variable results. However, use of the selection buffer, which contains 5 mM potassium, and annealing the samples to 60 °C provided reproducible results. A thorough search of experimental conditions was not performed. However, from the examination of samples from which potassium was not rigorously excluded, two forms of the aptamer were observed, one of which is the structure found in the presence of the selection buffer. In the presence of the selection buffer no concentration dependence of the NMR properties was observed.

NMR spectra were obtained using Varian XL-400 and VXR-400 spectrometers as well as a Bruker AM-600 located at the NIH Regional Resource at the University of Wisconsin, Madison. Phase-sensitive 600-MHz NOESY experiments at 100- and 250-ms mixing times in D_2O were collected into 1024 complex points in t_2 and 800 increments of t_1 with a spectral width of 6024.1 Hz and a recycle delay of 1.3 s, and 48 transients were obtained for each increment of the evolution time following two dummy scans. The 250-ms 600-MHz NOESY in H_2O were recorded with a spectral width of 13157.9 Hz, 1024 complex points in t_2, and 490 increments of t_1, and 64 transients were obtained for each increment of the mixing time. TOCSY experiments at 600 MHz were acquired into 1024 complex points in t_2 and 774 increments of t_1 with a mixing time of 51 ms, and 48 transients were averaged for each increment of the mixing time. The TOCSY data are not shown and were used to confirm assignments based on the NOESY data.

The free induction decays in both dimensions were multiplied by a 90°-shifted sine square bell weighting. The two-dimensional spectra were zero-filled to 2048 by 2048 real points. FELIX and Varian VNMR software were used for the data processing.

One-dimensional ^{31}P NMR spectra were obtained at 161.9 MHz with proton decoupling. The spectral width was 3271.2 Hz with 6016 complex points and 1024 scans.

Optical melting curves were obtained using a Hewlett-Packard UV/vis diode array spectrophotometer equipped with the Hewlett-Packard variable-temperature accessory. The optical melting curves were obtained at 260 nm with the DNA sample in the same buffer as used for the NMR experiments.

A preliminary structure for the aptamer was generated using the NOE volumes as distance constraints. The NOE cross-peak volumes were categorized as strong, medium, and weak to represent distance ranges (Clore & Groneneborn, 1989). These constraints were used to construct the structures for the G-G, T-T, and T-G-T fragments. These fragments were then connected to obtain an initial structure for the aptamer. A Dreiding II force field (Mayo et al., 1990) was then set up for the molecule which included 2.5 kcal/Å^2 constraints for the hydrogen bonds of the G quartets. Thus, each G quartet was modeled with eight hydrogen bond and eight torsional angle constraints. There were 34 additional distance constraints which were each assigned a force constant of 5 kcal/Å^2. The initial structure was then subjected to 100 steps of conjugate energy minimization, followed by 25 ps of microcanonical dynamics and then by an additional 100 steps of conjugate energy minimization.

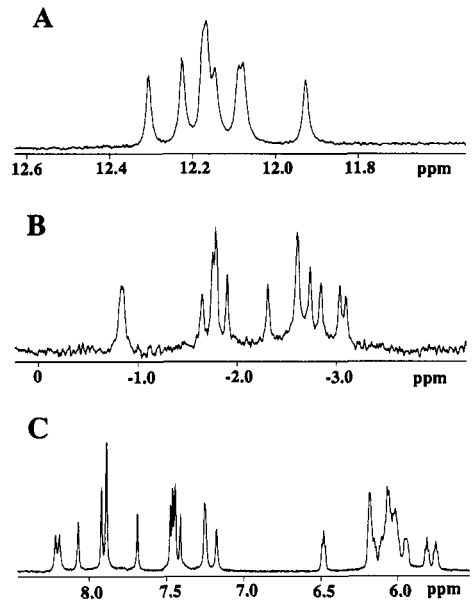

FIGURE 1: (A) The spectrum is the 600-MHz imino proton spectrum of the aptamer obtained at 10 °C. All NMR samples of the aptamer were at a concentration of 150 OD_{260} in the selection buffer containing 0.14 M NaCl, 20 mM perdeuteriated Tris, and 5 mM potassium chloride at a pH of 7.4. The preliminary characterization of the aptamer by NMR gave variable results. However, use of the selection buffer, which contains 5 mM potassium, and annealing the samples to 60 °C provided reproducible results. (B) The spectrum is the 161-MHz ^{31}P spectrum of the aptamer obtained at 10 °C. (C) The spectrum is the 600-MHz proton spectrum of the aptamer in ^2H_2O showing the region containing the H8 and H6 signals, 7–8.5 ppm, and the region containing the H1′ signals, 5.5–6.6 ppm.

The final structure, which is shown in Figure 5, was then used to predict the experimental NOE cross-peak volumes by solving the complete relaxation matrix assuming a 3-ns overall motion correlation time. The predicted and experimental NOE cross-peak volumes were found to be in good general agreement.

RESULTS AND DISCUSSION

The structural characterization of the aptamer began with obtaining the imino proton spectrum to determine the extent of base pairing (Van de Ven & Hilbers, 1988; Clore & Gronenborn, 1989; Wüthrich, 1986). The imino proton spectrum shown in Figure 1A indicates the presence of eight imino protons which are slowly exchanging with water. The examination of the imino proton region as a function of temperature showed that the aptamer melts at about 50 °C. By way of contrast, the hypochromicity at 260 nm was very small, in agreement with studies on telomere DNA sequences (Sen & Gilbert, 1990; Henderson et al., 1987). The hypochromicity for the DNA aptamer was too small to allow an accurate optical melting temperature to be determined.

The exchange rates of the imino protons with water were determined by partially drying a sample in water and reconstituting the sample in ^2H_2O. Periodic examination of the imino proton spectrum showed that the imino protons exchange very slowly. After one month the imino protons had not been exchanged. This very slow exchange has been previously noted for nucleic acids containing G tetrads (Smith & Feigon, 1992; Wang & Patel, 1992). The slow exchange rate is most likely due to a large entropic barrier associated with a cooperative opening of the aptamer structure in contrast to the breathing of duplex DNA.

The well-resolved ^{31}P spectrum shown in Figure 1B indicates that the backbone is distorted at several places as indicated

Table I: ^{31}P Chemical Shifts of d($G_1G_2T_3T_4G_5G_6T_7G_8T_9G_{10}G_{11}T_{12}T_{13}G_{14}G_{15}$) at 10 °C Relative to PO_4 at pH 7.0[a]

$\underline{G}_1$	G_2	T_3	T_4	$\underline{G}_5$	G_6	T_7	G_8	T_9	$\underline{G}_{10}$	G_{11}	T_{12}	T_{13}	$\underline{G}_{14}$
−2.85	−0.83	−1.66	−1.80	−2.74	−1.76	−2.32	−2.62	−3.11	−3.05	−0.85	−1.80	−1.91	−2.62

[a] Syn G residues are indicated by $\underline{G}$. The assignments of T_3, T_4, T_{12}, and G_{14} are tentative.

by the relatively wide range of ^{31}P chemical shifts (Van de Ven & Hilbers, 1988; Clore & Gronenborn, 1989; Wüthrich, 1986). It is noted that Z-DNA, which has alternating syn and anti residues (Wang et al., 1979), has downfield-shifted ^{31}P resonances (Van de Ven & Hilbers, 1988). Most of the ^{31}P resonances of the aptamer have been assigned by the combination of phosphorothioate labeling and ^{31}P–^1H heteronuclear correlation experiments, and the assignments are given in Table I.

The one-dimensional proton NMR spectrum, shown in Figure 1C, shows that only one form of the aptamer is present in solution since there are 15 signals from the nine G H8 and six T H6 protons in the aromatic region. The observed chemical shifts are suggestive of an unusual structure. The qualitative structural information obtained from the one-dimensional experiments suggests that the aptamer adopts an anomalous structure in solution.

The proton spectrum of the aptamer was assigned on the basis of NOESY, DQCOSY, and TOCSY data obtained at 400 and 600 MHz (Van de Ven & Hilbers, 1988; Clore & Gronenborn, 1989; Wüthrich, 1986; Ernst et al., 1987). More than 60 interresidue and 120 intraresidue NOEs were available to make the assignments. The NOESY data demonstrated that four of the G residues are in the syn conformation since the G H8–H1′ intraresidue NOEs of these residues are very strong as shown in Figure 2A. Therefore, assignments had to be made for 5′-anti–3′-anti, 5′-anti–3′-syn, and 5′-syn–3′-anti linkages. In 5′-anti–3′-anti linkages there are typically 5′ H1′, H2′ to 3′ H8/6 NOEs, and in 5′-syn–3′-anti there are 5′ H1′, H2′, H3′ to 3′ H6/8 NOEs (8–10). Interresidue NOEs are typically weak for 5′-anti–3′-syn linkages (Van de Ven & Hilbers, 1988; Clore & Gronenborn, 1989; Wüthrich, 1986).

The NOESY data on the sample in normal water showed that a single T methyl has NOEs to four different imino protons as the results in Figure 3A show. The NOESY results on the sample in normal water also showed that there were no strong imino–imino NOEs, which indicates that there are no G-T wobble pairs in the sample. Therefore, at the start of the assignment process there was evidence for G-G-G-G tetrads; one of the T residues is spatially close to a G-G-G-G tetrad, and four of the G residues are syn.

The spectra were assigned using NOESY data such as that in Figures 2 and 3. The cross-peaks between the aromatic and H2′/H2″ protons are shown in Figure 3B, and the cross-peaks between the aromatic and H1′ protons are shown in Figure 2B. There are two strings of 5′ G-G-T-T 3′ connectivities, which are $\underline{G}_1$-G_2-T_3-T_4 and $\underline{G}_{10}$-$\underline{G}_{11}$-T_{12}-T_{13}. Syn G residues are designated by $\underline{G}$. Two additional 5′ G-G 3′ connectivities are shown between $\underline{G}_{14}$-G_{15} and $\underline{G}_5$-$\underline{G}_6$. The other cross-peaks have also been assigned but are not labeled in these figures. Two stretches of 5′ GTT 3′ residues could also be identified on the basis of anti–anti connectivities. These two- to four-residue stretches of sequential connectivities were arranged using the information in long-range NOE connectivities.

Unlike the case of duplex DNA there are a number of NOE connectivities observed for the aptamer between residues which are not adjacent in sequence. In particular, NOEs are observed between the H8 of G_2 and the methyl, H2′, and H2″ protons

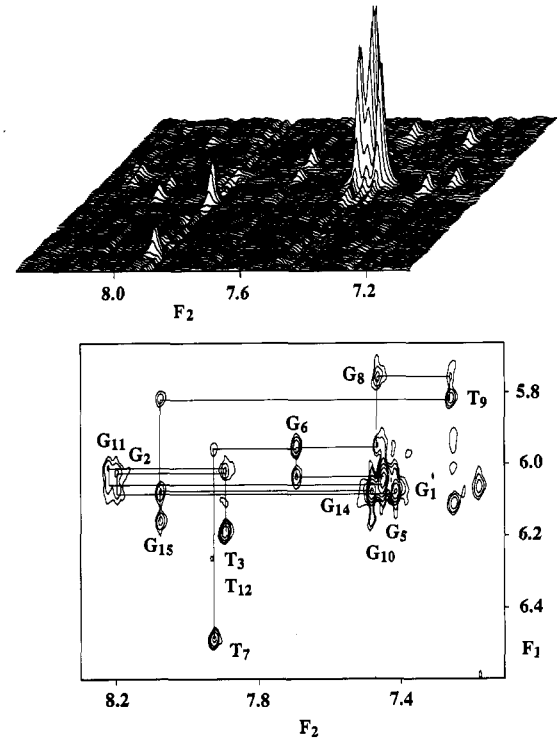

FIGURE 2: (A, top) The spectrum shown is a portion of the 600-MHz NOESY spectrum obtained with a mixing time of 250 ms at 10 °C. The cross-peaks are between H8/H6 and H1′ protons, and the vertical axis is from 5.7 to 6.6 ppm. The stacked mode presentation shows the higher intensities of the cross-peaks of the syn residues. (B, bottom) The same spectrum is shown in the contour plot mode of display. The connectivities of most interest are shown, and the assignments of the cross-peaks are indicated.

of T_4 and between the H8 of G_{11} and the methyl, H2′, and H2″ of T_{13}. Complementary information is provided by the NOEs from the methyl of T_4 to the H1′, H2′, and H2″ of G_2 and from the methyl of T_{13} to the H1′, H2′, and H2″ of G_{11}. In addition, there are NOEs between the H2″ of T_4 and a G imino proton and between the H2″ of T_{13} with a different G imino proton. These imino protons are not the same as those which have NOEs to the residues of the TGT loop. This collection of NOEs places the T_4 and T_{13} residues close to the G_2-$\underline{G}_5$-G_{11}-$\underline{G}_{14}$ tetrad.

There are also NOE connectivities between the H8 of G_8 and the H1′, H2′, and H2″ protons of G_6 and between the H1′ of T_9 and the H8 of G_{15}. These NOEs are in conjunction with the NOEs of the methyl of T_9 to the imino protons of $\underline{G}_1$, G_6, $\underline{G}_{10}$, and G_{15}. There are also NOEs between the H1′ proton of G_8 and the H1′ proton of T_9 with G imino protons as shown in Figure 3A. This collection of long-range NOEs places severe constraints on the possible structures of the TGT loop of the aptamer.

Taken together, these results showed that the primary structure of the aptamer is $\underline{G}GTT\underline{G}GTGT\underline{G}GTT\underline{G}G$, and the assignments of the proton resonances are given in Table II. The incorporation of the NOEs from the TGT region to the $\underline{G}GTT$ regions confirmed the orientation of the loop to the rest of the molecule as well as allowing a single T methyl to have NOE connectivities to four distinct imino protons.

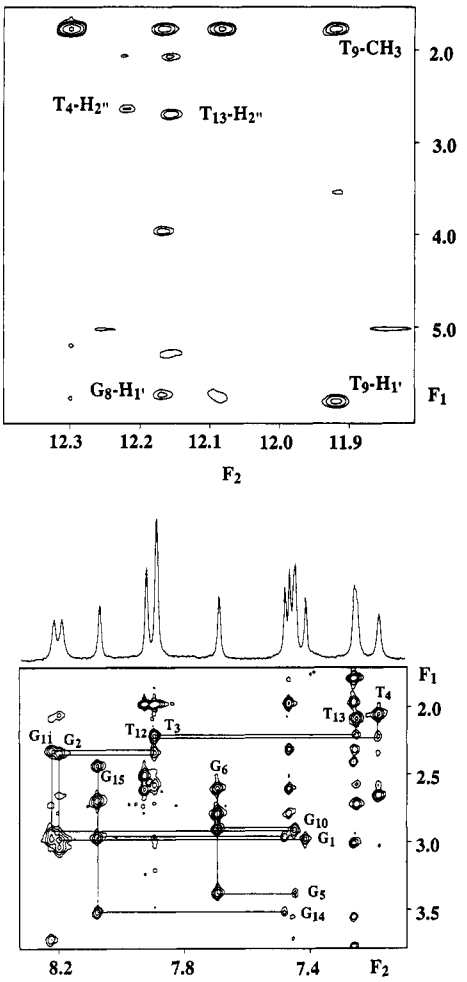

FIGURE 3: (A, top) The contour plot shown is a portion of a 600-MHz NOESY spectrum obtained with a mixing time of 250 ms. The cross-peaks are between the imino protons and the methyl, H1′, H2′, and H2″ protons. The key connectivities are indicated. The methyl of T9 has NOE connectivities to four distinct imino protons, the H2″ protons of T13 and T4 have connectivities of imino protons (not the same iminos as the T9 methyl), and the H1′ protons of G8 and T9 also have NOE connectivities to imino protons which are the same iminos as those which have NOE connectivities to the T9 methyl. (B, bottom) The contour plot shown is a portion of a 600-MHz NOESY spectrum obtained with a mixing time of 250 ms showing the aromatic to H2′/H2″ cross-peaks. The key connectivities are indicated, and the assignments of the cross-peaks are given.

To arrive at the three-dimensional structure, all possible structures which included two syn–anti–syn–anti G tetrads, to be consistent with the imino proton data, and which had the 5′ GG 3′ alternating between syn and anti, to be consistent with the NOE and other NMR data, were considered. Only one folding pattern was found to be consistent with all of the NOE connectivities, and this tertiary structure is shown in Figure 4 along with a depiction of a G tetrad. The tertiary structure, shown in Figure 4A, was constructed by use of the interresidue NOEs with particular use of the NOEs between residues not adjacent in sequence. This is a new structural motif for DNA which has not been previously documented. Some of the key NOEs are those from the methyl of T_9 to four distinct imino protons and the H1′ of T_9 to the H8 of G_{15}. The H8 of G_8 has NOEs to several sugar protons of G_6. These NOEs place G_8 and T_9 near the $\underline{G}_1$-G_6-$\underline{G}_{10}$-G_{15} tetrad. The methyl of T_{13} has NOEs to the H8, H1′, H2′, and H2″ of G_{11}, and the methyl of T_4 has NOEs to the H8, H1′, H2′, and H2″ of G_2. In addition, the H2′ and H2″ of T_4 and T_{13} have NOE connectivities to imino protons, which are not the iminos connected to T_9.

This structure for the aptamer is highly compact, has G-G-G-G tetrads which are syn–anti–syn–anti, has a loop partially folded over the $\underline{G}_1$-G_6-$\underline{G}_{10}$-G_{15} tetrad, and has T_3, T_4, T_{12}, and T_{13} under the $\underline{G}_2$-$\underline{G}_5$-$\underline{G}_{11}$-$\underline{G}_{14}$ tetrad. This model is consistent with all of the NMR results, with the consensus sequence for thrombin binding and that GGTTGG also binds to and inhibits thrombin (Bock et al., 1992). A dimer of GGTTGG could form a structure similar to that adopted by the aptamer with the exception of the TGT loop.

A preliminary NMR resolution structure for the aptamer is shown in Figure 5 from two perspectives. This structure was obtained, as described above, from the combined use of the NOE data and molecular modeling. The view in Figure 5A is essentially that of Figure 4A and illustrates the compact nature of the aptamer structure. The view shown in Figure 5B shows that the backbone of the aptamer contains essentially four straight segments connected by the three loops. This view also indicates a low level of helicity for the backbone.

The NMR results also support the notion that the structure of the aptamer determined here is essentially the same as that which binds to thrombin. The imino exchange rates indicate that the structure is stable on the time scale of weeks to months. Since the binding to thrombin occurs many orders of magnitude faster than this with a large binding constant, it is difficult to construct a reasonable model which has the aptamer undergoing a large conformational change upon binding. For a large conformational change to occur, the binding of the aptamer to thrombin must be accompanied by an efficient catalysis of the opening up of the aptamer structure. Preliminary ^{31}P NMR results on the one-to-one complex of the aptamer with thrombin indicate that the ^{31}P spectrum of the aptamer does not undergo significant change upon binding to thrombin. This preliminary result supports the notion that the aptamer does not undergo significant conformational change upon binding to thrombin.

The four syn G residues all have resonances in the upfield region as indicated in Table I. The ^{31}P chemical shifts of the phosphates between syn and anti residues of this DNA aptamer are in contrast with the results on the syn–anti steps of Z-DNA (Van de Ven & Hilbers, 1988; Feigon et al., 1985). In Z-DNA the chemical shifts of the syn G–phosphate–anti C sites are observed to be downfield shifted relative to those of the anti–syn sites of Z-DNA and of the anti–anti sites of B-DNA (Van de Ven & Hilbers, 1988; Feigon et al., 1985). The results on the aptamer indicate that the ^{31}P chemical shift is not necessarily diagnositic of syn–anti sites in DNA.

There have been a number of investigations of the NMR (Hardin et al., 1991, 1992; Wang et al., 1991; Henderson et al., 1987; Smith & Feigon, 1992; Wang & Patel, 1992), UV (Hardin et al., 1991, 1992; Sen & Gilbert, 1990; Henderson et al., 1990), CD (Guschlbauer et al., 1990; Hardin et al., 1991; Zahler et al., 1991), gel electrophoresis (Guschlbauer et al., 1990; Hardin et al., 1991; Williamson et al., 1989; Sen & Gilbert, 1988, 1990; Sundquist & Klug, 1989), nuclease sensitivity (Voloshin et al., 1992; Blackburn, 1991), photo-cross-linking (Williamson et al., 1989), chemical protection (Williamson et al., 1989; Henderson et al., 1987), and potassium dependence (Guschlbauer et al., 1990; Hardin et al., 1991, 1992; Williamson et al., 1989; Sen & Gilbert, 1990; Wang et al., 1991; Henderson et al., 1987; Zahler et al., 1991; Kang et al., 1992; Wang & Patel, 1992; Smith & Feigon, 1992) of the properties of DNAs containing the general sequence G_mT_n. A prime motivation for these studies on tetraplexes arises from G_mT_n sequences being found in eukaryotic telomeres (Blackburn, 1991). It has been proposed

Table II: Proton Assignments of d($G_1G_2T_3T_4G_5G_6T_7G_8T_9G_{10}G_{11}T_{12}T_{13}G_{14}G_{15}$)[a]

	H6/H8	H1′	H2′	H2″	H3′	H4′	H5′/H5″	CH_3
$\underline{G}_1$	7.42	6.08	2.96	2.96	4.99	4.40	4.03/4.12	
$\underline{G}_2$	8.20	6.03	3.04	2.34	5.15	4.41	4.23	
T_3	7.90	6.19	2.22	2.56	4.91	4.29	4.24/4.32	1.98
T_4	7.18	6.07	2.06	2.66	4.88	4.20	3.92	1.03
$\underline{G}_5$	7.45	6.04	3.38	2.91	4.87	4.41	4.23/4.28	
G_6	7.70	5.95	2.79	2.61	5.12	4.45	4.23	
T_7	7.93	6.49	2.51	2.61	4.86	4.43	4.24/4.28	1.98
G_8	7.47	5.77	1.98	2.32	4.77	3.98	4.01/4.10	
T_9	7.26	5.82	1.96	2.41	4.62	3.76	3.01/3.55	1.79
$\underline{G}_{10}$	7.46	6.06	3.72	2.93	4.92	4.28	4.14	
G_{11}	8.23	6.02	2.98	2.33	5.14	4.39	4.22	
T_{12}	7.90	6.19	2.20	2.58	4.91	4.29	4.24/4.32	1.98
T_{13}	7.25	6.11	2.08	2.72	4.90	4.22	3.92	0.98
$\underline{G}_{14}$	7.48	6.08	3.51	2.96	4.92	4.42	4.30/4.37	
G_{15}	8.08	6.16	2.69	2.44	4.80	4.25	4.12/4.18	

[a] Syn G residues are indicated by G. The HDO signal is referenced at 4.93 ppm at 10 °C.

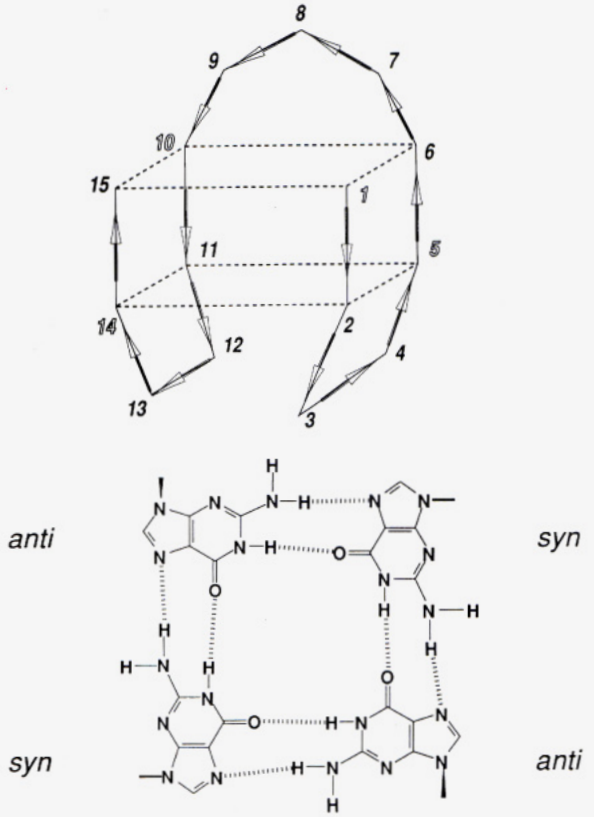

FIGURE 4: (A, top) A depiction of the tertiary structure of the aptamer is shown. The residue numbers in outline format indicate a syn residue, and the dashed lines indicate the locations of the G tetrads. The direction of the backbone is indicated by the arrows. (B, bottom) A depiction of a syn–anti–syn–anti tetrad is shown.

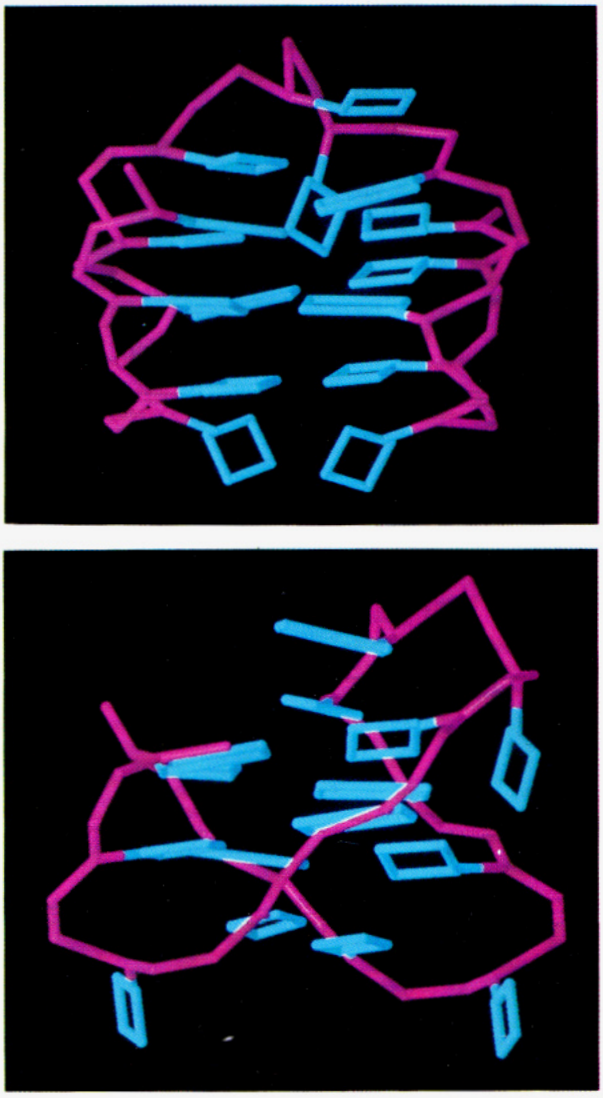

FIGURE 5: (A, top) A preliminary model of the aptamer structure has been built, which is shown in the same orientation as in Figure 4A. In this depiction the bases are shown as blue rectangles, and the backbone is shown as connected pink cylinders. This structure exhibits no strongly unfavorable contacts and agrees well with the experimental NMR data. (B, bottom) The model of the aptamer structure is shown in an orientation to illustrate both the nonplanarity of the G tetrads and the orientation of the backbone.

that the presence of tetraplex structures in telomers may protect the ends of chromosomes as well as conferring other properties (Blackburn, 1991).

Of particular interest is the crystal structure of d(GGGGTTTTGGGG), which is the telomere DNA from *Oxytricha*, recently determined by Rich and co-workers (Kang et al., 1992). The G tetrads in the crystal structure are anti–syn–anti–syn, the 5′ GG 3′ alternate between syn and anti, and the structure contains potassium. These are the same basic structural features observed for the tetrads of the aptamer in solution. Since our results show that a syn–anti–syn–anti tetrad does form in solution, and is stabilized by potassium, as are the telomere structures, it appears that the aptamer structure has structural features similar to those adopted by some telomere DNAs. However, the *Oxytricha* crystal structure arises from dimers of DNA and has two loops, whereas the aptamer is a monomer and has three loops. The

three-loop aptamer structure is reminiscent of ones proposed by Cech and co-workers for single-stranded telomere DNA (Hardin et al., 1991; Zahler et al., 1991), and the three-loop structural motif may be that which telomere DNA actually adopts. An intramolecular, three-loop structure is consistent with the existing data on telomere DNA (Hardin et al., 1991; Zahler et al., 1991), but dimer structures are not.

The aptamer structure reported here and the *Oxytricha* crystal structure results are distinct from a structure of d(GGGGTTTTGGGG) proposed on the basis of NMR results which has G-G-G-G tetrads which are syn–syn–anti–anti (Smith & Feigon). Both the NMR and crystal studies on *Oxytricha* were on dimers. A study on a tetramer containing G tetrads suggested that the G residues in the tetrads are all anti and the four strands of the tetramer are parallel (Wang & Patel, 1992). It is noted that the proposed parallel arrangement of the strands in the tetramers cannot be relevant to the tetrad structures formed by intramolecular association of telomere DNA observed by Cech and co-workers (Hardin et al., 1991; Zahler et al., 1991).

It was unexpected that the structure of telomere DNA and an aptamer which binds to and inhibits thrombin may have similar structural features. This remarkable coincidence suggests that this aptamer may have interesting interactions with the proteins responsible for synthesizing and stabilizing telomere structure and that this structural motif may be useful in inhibiting enzymes other than thrombin. This similarity also indicates that the tetrad structure may turn out to be a basic structural element of DNA and may be found in aptamers to targets other than thrombin as well as in naturally occurring systems other than telomeres.

ACKNOWLEDGMENT

The assistance of Drs. I. Goljer and J. M. Withka at the preliminary stages of this project is acknowledged. The 600-MHz spectra were obtained with the assistance of Dr. Frits Abildgaard using the NMR facility at the University of Wisconsin, Madison, which is supported by NIH Grant RR02301 with equipment purchased with support from the University of Wisconsin, NSF DMB-8415048, NIH RR02781, and the USDA.

REFERENCES

Blackburn, E. (1991) *Nature 350*, 569–573.

Bock, L. C., Griffin, L. C., Latham, J. A., Vermaas, E. H., & Toole, J. J. (1992) *Nature 355*, 564–566.

Clore, G. M., & Gronenborn, A. M. (1989) *CRC Crit. Rev. Biochem. Mol. Biol. 24*, 479–564.

Eckstein, F., & Jovin, T. M. (1983) *Biochemistry 22*, 4546–4550.

Ellington, A. D., & Szostak, J. W. (1990) *Nature 346*, 818–822.

Ernst, R. R., Bodenhausen, G., & Wokaun, A. (1987) *Principles of NMR in One- and Two-Dimensions*, Oxford University Press, Cambridge.

Feigon, J., Wang, A. H.-J., Van der Marel, G. A., Van Boom, J. H., & Rich, A. (1985) *Science 230*, 82–84.

Guschlbauer, W., Chantot, J.-F., & Thiele, D. (1990) *J. Biomol. Struct. Dyn. 3*, 491–511.

Hardin, C. C., Henderson, E., Watson, T., & Prosser, J. K. (1991) *Biochemistry 30*, 4460–4472.

Hardin, C. C., Watson, T., Corregan, M., & Bailey, C. (1992) *Biochemistry 31*, 833–841.

Henderson, E., Hardin, C. C., Walk, S. K., Tinoco, I., & Blackburn, E. H. (1987) *Cell 51*, 899–908.

Henderson, E. R., Moore, M., & Malcolm, B. A. (1990) *Biochemistry 29*, 732–737.

Kang, C., Zhang, X., Ratliff, R., Moyzis, R., & Rich, A. (1992) *Nature 356*, 126–131.

Mayo, S. L., Olafson, B. D., & Goddard, W. A., III (1990) *J. Phys. Chem. 94*, 8897–8909.

Salzman, E. W. (1992) *N. Engl. J. Med. 326*, 1017–1019.

Sen, D., & Gilbert, W. (1988) *Nature 334*, 364–366.

Sen, D., & Gilbert, W. (1990) *Nature 344*, 410–414.

Smith, F. W., & Feigon, J. (1992) *Nature 356*, 164–168.

Sundquist, W. I., & Klug, A. (1989) *Nature 342*, 825–829.

Van de Ven, F. J. M., & Hilbers, C. W. (1988) *Eur. J. Biochem. 178*, 1–38.

Voloshin, O. N., Vaselkov, A. G., Belotserkovskii, B. P., Danilevskaya, O. N., Pavolova, M. N., Dobrynin, V. N., & Frank-Kamenetskii, M. D. (1992) *J. Biomol. Struct. Dyn. 9*, 643–652.

Wang, A. H.-J., Quigley, G. J., Kolpak, F. J., Crawford, J. L., van Boom, J. H., van der Marel, G., & Rich, A. (1979) *Nature 282*, 680–686.

Wang, Y., & Patel, D. J. (1992) *Biochemistry 31*, 8112–8119.

Wang, Y., Jin, R., Gaffney, B., Jones, R. A., & Breslauer, K. J. (1991) *Nucleic Acids Res. 19*, 4619–4622.

Williamson, J. R., Raghuraman, M. K., & Cech, T. R. (1989) *Cell 59*, 871–880.

Wüthrich, K. (1986) *NMR of Proteins and Nucleic Acids*, Wiley, New York.

Zahler, A. M., Williamson, J. R., Cech, T. R., & Prescott, D. M. (1991) *Nature 350*, 718–720.